



## Structural and ferroelectric properties in the solid solution $(\text{Ba}_5\text{TbTi}_3\text{V}_7\text{O}_{30})_x(\text{BiFeO}_3)_{1-x}$

Hage Doley, Pratap Kumar Swain, Anuradha Panigrahi & Gyati Tachang Tado

To cite this article: Hage Doley, Pratap Kumar Swain, Anuradha Panigrahi & Gyati Tachang Tado (2020) Structural and ferroelectric properties in the solid solution  $(\text{Ba}_5\text{TbTi}_3\text{V}_7\text{O}_{30})_x(\text{BiFeO}_3)_{1-x}$ , Ferroelectrics, 568:1, 104-111, DOI: [10.1080/00150193.2020.1811034](https://doi.org/10.1080/00150193.2020.1811034)

To link to this article: <https://doi.org/10.1080/00150193.2020.1811034>



Published online: 03 Nov 2020.



Submit your article to this journal [↗](#)



Article views: 8



View related articles [↗](#)



View Crossmark data [↗](#)



# Structural and ferroelectric properties in the solid solution (Ba<sub>5</sub>TbTi<sub>3</sub>V<sub>7</sub>O<sub>30</sub>)<sub>x</sub>(BiFeO<sub>3</sub>)<sub>1-x</sub>

Hage Doley<sup>a</sup>, Pratap Kumar Swain<sup>a</sup>, Anuradha Panigrahi<sup>b</sup>, and Gyati Tachang Tado<sup>b</sup>

<sup>a</sup>Department of Physics, National Institute of Technology, Arunachal Pradesh, Yupia, India; <sup>b</sup>Department of Physics, Dera Natung Govt. College, Itanagar, India

## ABSTRACT

The solid solution of (Ba<sub>5</sub>TbTi<sub>3</sub>V<sub>7</sub>O<sub>30</sub>)<sub>x</sub>(BiFeO<sub>3</sub>)<sub>1-x</sub> has been synthesized by solid-state reaction technique with different *x* values. XRD (X-Ray Diffractogram) study confirms the formation of single-phase compound for *x* = 1. Grain morphology has been studied by Scanning electron microscope (SEM: JOEL-IT300). By Impedance Analyzer (HIOKI-IM3536) dielectric properties such as dielectric constant and loss tangent have been measured in a wide temperature range (RT–500° C) and also with a wide range of frequency (1 kHz–1 MHz). This dielectric result confirms the Ferroelectric nature of all the samples and with increasing content of BiFeO<sub>3</sub>, the dielectric constant decreases.

## ARTICLE HISTORY

Received 25 September 2019  
Accepted 31 January 2020

## KEYWORDS

Solid solution; ferroelectric; dielectric constant; loss tangent and impedance analyzer

## 1. Introduction

The rare-earth doped barium niobate-titanate compound Ba<sub>5</sub>RTi<sub>3</sub>Nb<sub>7</sub>O<sub>30</sub> (R: Rare Earth Element) of TB structure [1] has been widely studied and found out to be a good ferroelectrics material, and it has diverse application ranging from a small but ubiquitous capacitor, transistors, memories to extremely sophisticated piezoelectric systems. By changing the R in BRTN, we get a wide range of variation in T<sub>c</sub> (Curie Temperature) [2] and this materials also shows the diffused phase transitions which could be explored in various ways. However, the problem with this barium niobate-titanate is that the Calcination temperature is found to be very high.

Literature survey shows that in Ba<sub>5</sub>RTi<sub>3</sub>Nb<sub>7</sub>O<sub>30</sub> when Nb (Niobium) is replaced by V (Vanadium) of a lower atomic radius of same periodic group the calcination and sintering temperature was found to reduce drastically [3, 4] without compromising its ferroelectrics properties. Researchers also found that substitution of V enhances the thermal stability, low value of leakage current [5] and improved dielectric and ferroelectric properties [6–8] though different R (Rare earth) have been used by researchers there is no report about Terbium (Tb). So in our present work, we study the ferroelectrics properties of Ba<sub>5</sub>TbTi<sub>3</sub>V<sub>7</sub>O<sub>30</sub> with R = Tb (Terbium).

Some of the materials have both the electric and magnetic ordering, which is known as multiferroic material popularly known as smart materials [9]. The coexistence of

different orders could be utilized for the development of spintronic devices, dual storage devices and sensors [10]. Bismuth Ferrite ( $\text{BiFeO}_3$ ) is one of such multiferroic material which has been widely studied having Neel Temperature  $\sim 643$  K and Curie Temperature  $\sim 1100$  K [11, 12] having rhombohedrally distorted perovskite structure [13, 14]. Because of its superstructure and semiconducting nature at room temperature it does not allow proper electrical poling and leads to high dielectric loss [15] and hence low dielectric constant

In our present work, we have prepared the solid solution of the multiferroic materials,  $\text{BiFeO}_3$  with the ferroelectrics materials,  $\text{Ba}_5\text{TbTi}_3\text{V}_7\text{O}_{30}$  in suitable proportion. The aim of the work is to study the effect of BFO on the ferroelectric properties of BTTV and also at the same time to see the effect of BTTV on the ferroelectric properties of BFO

## 2. Material preparation

Raw materials of  $\text{BaCO}_3$ ,  $\text{Tb}_2\text{O}_3$ ,  $\text{V}_2\text{O}_5$  were taken for the preparation of a polycrystalline sample of  $\text{Ba}_5\text{TbTi}_3\text{V}_7\text{O}_{30}$  (BTTV). In stoichiometric ratio, these compound are thoroughly ground in an agate mortar in the wet environment of methanol which is then calcined in a muffle furnace at a temperature of  $\sim 1023$  K. Which is then further ground to a fine form and then checked in XRD to confirm whether the single-phase compound is formed. For the preparation of  $\text{BiFeO}_3$  (BFO) the materials  $\text{Fe}_2\text{O}_3$  and  $\text{Bi}_2\text{O}_3$  are taken in a stoichiometric ratio which is calcined at  $973$  K for 4 hrs. For the preparation of the solid solution  $(\text{Ba}_5\text{TbTi}_3\text{V}_7\text{O}_{30})_x(\text{BiFeO}_3)_{1-x}$ . The powder of  $\text{Ba}_5\text{TbTi}_3\text{V}_7\text{O}_{30}$  and  $\text{BiFeO}_3$  are mixed as per the requirements. The powder is die pressed by the hydraulic press of about pressure of  $\sim 100$  psi in the pallet form of size of  $\sim 13$  mm diameter and 1-2 mm thickness; the pallets are further sintered at  $\sim 1073$  K. The formation of the sample is confirmed by X-ray diffractogram (Rigaku, Miniflex) with  $\text{CuK}_\alpha$  radiation of wavelength  $= 1.5405 \text{ \AA}$  in the range of Bragg's angles  $2\theta (10^\circ \leq \theta \leq 60^\circ)$  with a scanning rate of  $3^\circ/\text{min}$ . Scanning electron microscope (SEM: JOEL-IT300) is employed for the study of surface morphology. The pallets are then made conducting by silver pasting on both sides for electrical measurement using Impedance Analyzer (HIOKI-IM3536).

## 3. Results and discussion

### 3.1. Structural study

The calcined powder has been put into X-ray Diffractogram (XRD) at room temperature for the structural characterization. Figure 1 shows a sharp and single diffraction peaks, which are the phase of BFO at the expected regions, which confirms the formation of single-phase compounds for  $x=1$ . For  $x=0.5$  and  $x=0.3$  there are additional peaks due to BFO which confirms the formation of a solid solution.

### 3.2. Microstructural study

Figure 2(a-c) shows the SEM micrographs of which show for  $x=1$ , 0.5 and 0.3, which shows that the grain growth is more or less complete. From Figure 2(a-c) by linear intercept method the average grain size of all the materials are measured

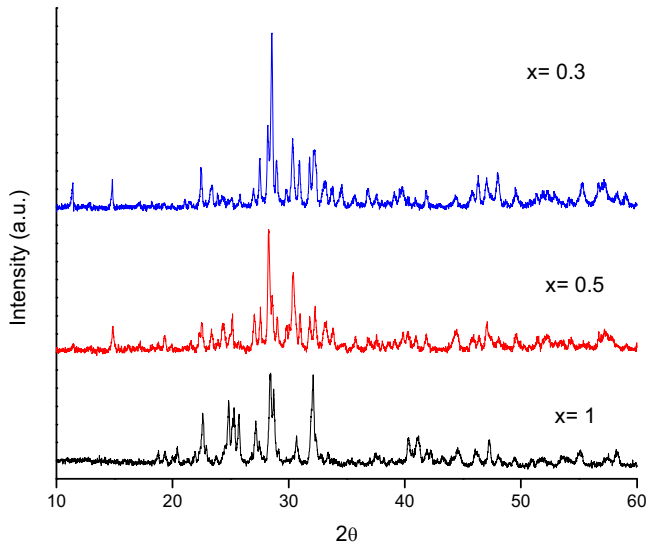


**Figure 1.** XRD pattern for  $(\text{BTTV})_x(\text{BFO})_{1-x}$ .

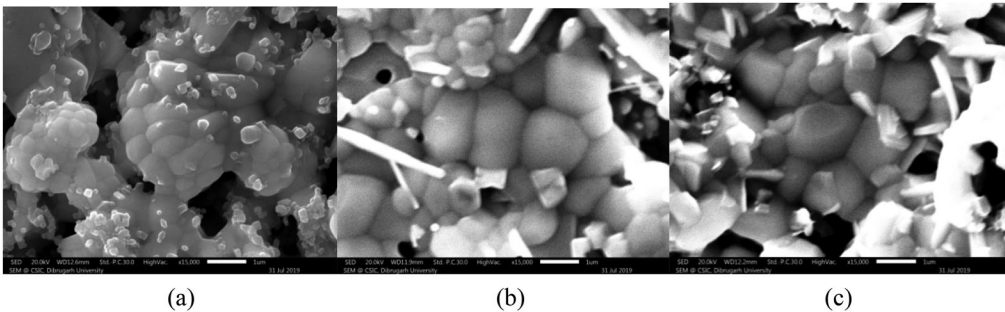


**Figure 2.** SEM micrographs of  $(\text{BTTV})_x(\text{BFO})_{1-x}$  (a)  $x=1$  (b)  $x=0.5$  (c)  $x=0.3$  at magnification of X 15,000.

- (i) For  $x=1$ : SEM micrograph of  $\text{Ba}_5\text{TbTi}_3\text{V}_7\text{O}_{30}$  shows that the average size is around  $0.89\ \mu\text{m}$ , the shape is of oval, elongated and angular shape.
- (ii) For  $x=0.5$ : SEM micrograph of  $(\text{Ba}_5\text{TbTi}_3\text{V}_7\text{O}_{30})_{0.5}(\text{BiFeO}_3)_{0.5}$  shows that the average size is around  $1.8\ \mu\text{m}$ . The shape is spherical and elongated. There is presence of porosity is distinctly visible in the compound also there is appearance of columnar shape grains.
- (iii) For  $x=0.3$ : SEM micrograph of  $(\text{Ba}_5\text{TbTi}_3\text{V}_7\text{O}_{30})_{0.3}(\text{BiFeO}_3)_{0.7}$  shows that the average size of the grain is  $\sim 1.36\ \mu\text{m}$ . The shape is more of cubicle and angular. The size of the grain decreases when BFO is increased, but the porosity also increases. The columnar shape grain becomes more distorted.

### 3.3. Dielectric studies

Figure 3 shows the frequency variation of  $\epsilon_r$  of  $(\text{BTTV})_x(\text{BFO})_{1-x}$  at room temp; it shows that with an increase in frequency from 1 kHz to 100 kHz, the  $\epsilon_r$  decreases for

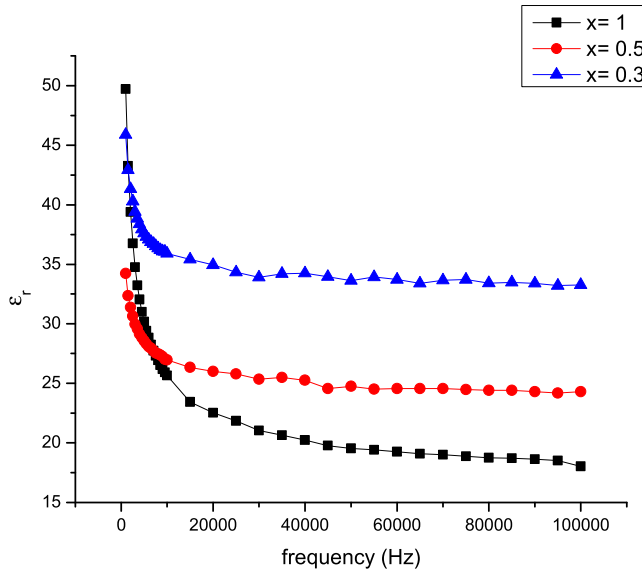


**Figure 3.** Frequency variation of  $\epsilon_r$  of  $(\text{BTTV})_x(\text{BFO})_{1-x}$  at room temp.

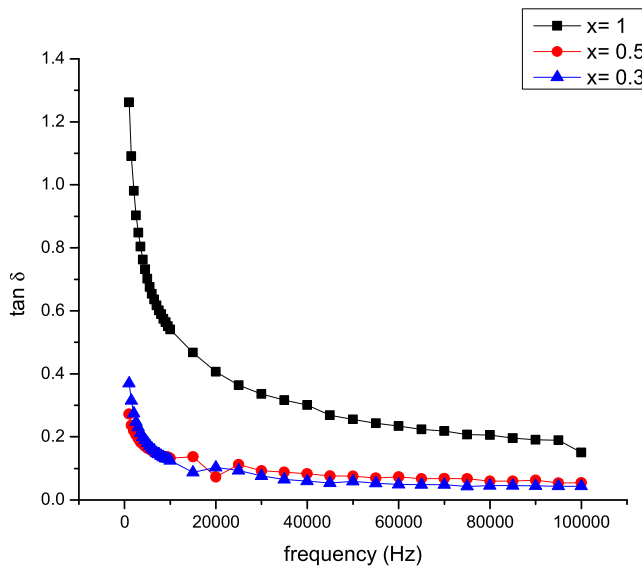


**Figure 4.** Frequency variation of  $\tan \delta$  of  $(\text{BTTV})_x(\text{BFO})_{1-x}$  at room temp.

$x=1$  from  $\sim 50$  to  $\sim 18$ , for  $x=0.5$  from  $\sim 34$  to  $\sim 24$  and for  $x=0.3$  from  $\sim 46$  to  $\sim 33$ , the trend we got is as expected of the dielectric materials i.e. with increase in frequency the dielectric constant decreases. It is seen that with addition of BFO the dependency of dielectric constant with frequency decreases.

Figure 4 shows the variation of  $\tan \delta$  with frequency for  $(\text{BTTV})_x(\text{BFO})_{1-x}$  at room temp, it shows that with increase in frequency from 1 kHz to 100 kHz, the  $\tan \delta$  decreases for  $x=1$  from  $\sim 1.25$  to  $\sim 0.18$ , for  $x=0.5$  from  $\sim 0.26$  to  $\sim 0.05$  and for  $x=0.3$  from  $\sim 0.36$  to  $\sim 0.045$ , the trend is as expected for dielectric materials. It can

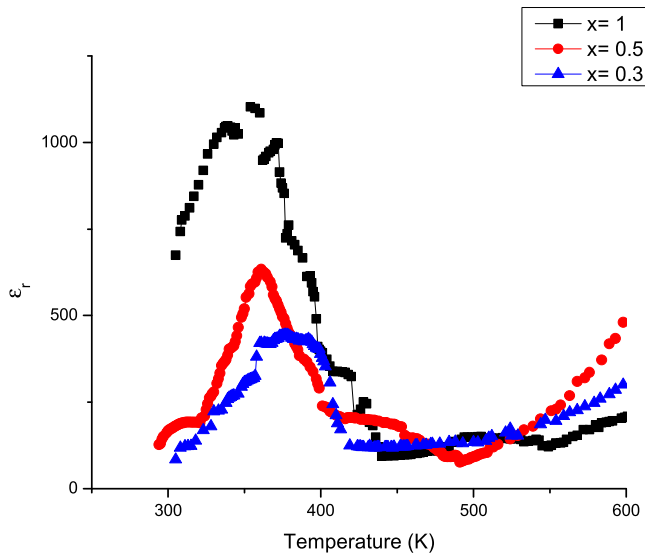


**Figure 5.** Variation of  $\epsilon_r$  with temperature for  $(\text{BTTV})_x(\text{BFO})_{1-x}$  at 1kHz.

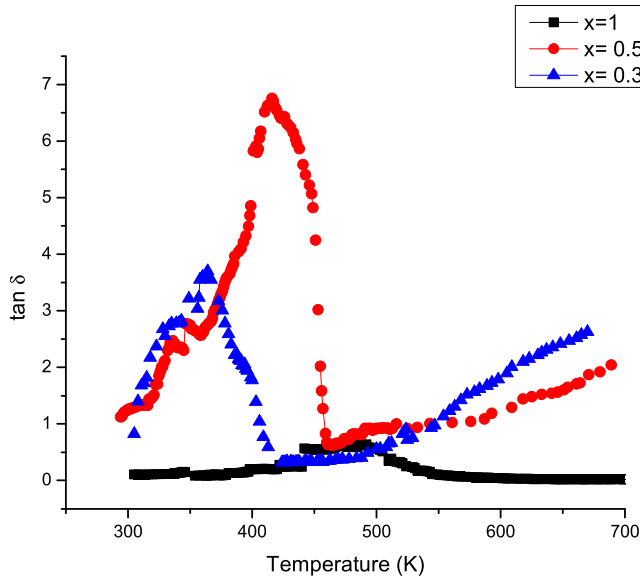
**Table 1.** Comparison of dielectric properties,  $T_c$ (K), and Activation Energy ( $E_a$ ) of  $(\text{BTTV})_x(\text{BFO})_{1-x}$  for different values of  $x$ .

$(\text{BTTV})_x(\text{BFO})_{1-x}$	$\epsilon_{RT}$	$\epsilon_{max}$	$T_c$	$E_a$
$x=1$	671	1100	356	0.05eV
$x=0.5$	157	631	361	0.331eV
$x=0.3$	84	439	378	0.3639eV

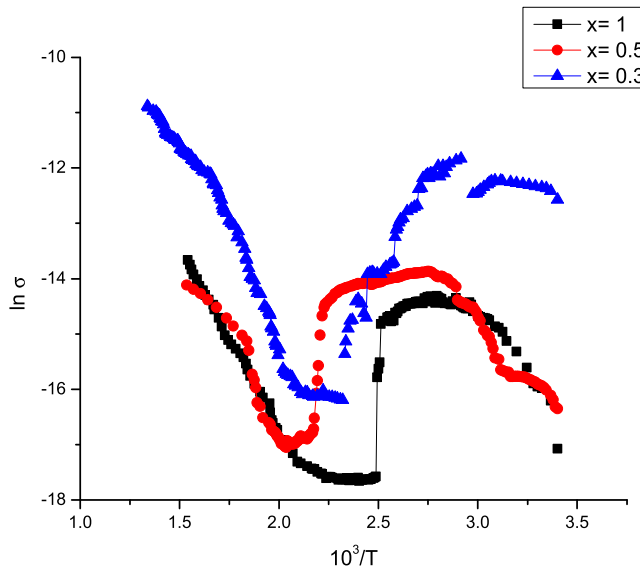
also be seen from the figure that when BFO is increased i.e. from  $x=0.5$  to 0.3, change in  $\tan\delta$  with frequency remain more or less same.

Figure 5 shows variation of dielectric constant  $\epsilon_r$  with temp in a wide range varying from room temperature to 500 °C for frequency at 1000 Hz. It has been observed that the dielectric constant ( $\epsilon_r$ ) at the beginning rises with temperature and at the transition temperature it reaches to the peak and then it decreases with further rise in temperature and after certain temperature the dielectric constant increase at the similar rate. It may be inferred that after certain temperature the addition of multiferroic BFO doesn't change the properties of the ferroelectric nature of solid solution and the material starts behaving as pure paraelectric materials. From the Table 1, it can be seen that for pure BTTV the dielectric constant ( $\epsilon_{max}$ ) is  $\sim 1100$  and when  $x=0.5$  i.e. 50% BFO is added the maximum dielectric constant reduces to the  $\sim 631$  which further reduces to  $\sim 377$  when  $x=0.3$  i.e. 70% BFO is added. From the table it can also be inferred that even at the room temperature pure ferroelectric has higher dielectric constant ( $\epsilon_{RT} \sim 671$ ) than that of maximum dielectrics of either of the composites.

Figure 6 shows variation of loss tangent  $\tan\delta$  with temp for  $(\text{BTTV})_x(\text{BFO})_{1-x}$  in a wide range of temperature varying from room temperature to 500 °C at 1000 Hz frequency. It has been observed that at the beginning loss tangent increases with the increase in temperature. The loss tangent is least when the pure ferroelectric material is considered i.e. for  $x=1$  and as the content of BFO increases the  $\tan\delta$  also increases but the maximum loss tangent is observed for  $x=0.5$  i.e. when it contains 50% BFO. And



**Figure 6.** Tangent loss with temperature for  $(\text{BTTV})_x(\text{BFO})_{1-x}$  at 1kHz.



**Figure 7.** Conductivity Study for  $(\text{BTTV})_x(\text{BFO})_{1-x}$  at 1kHz.

at higher temperature it is found that the loss tangent is dependent on the content of BFO, as the content of BFO increases the loss tangent also increases.

### 3.4. Conductivity study

The relation between ac conductivity and temperature is shown in Figure 7 for the frequency of 1kHz. The observed curve supports that electrical conductivity is the thermally activated transport properties and obeys Arrhenius equation:  $\sigma_{ac} = \sigma_o \exp(-E_a/$

$k_B T$ ) where ‘A’ is a constant, ‘ $E_a$ ’ is the activation energy and ‘ $k_B$ ’ is the Boltzmann’s constant [16]. The fig shows that in ferroelectric region the ac conductivity of the compound is increasing with the increase in the temperature and shows the negative temperature coefficient of resistance (NTCR) [17] behavior which is expected behavior ferroelectric materials. The activation energy increases as seen from the Table 1 i.e. from 0.05 eV for pure ferroelectric material to 0.331 eV to 0.3639 eV with the increase in the multiferroic BFO content. The increase in activation energy maybe is due to increase in the conduction of the solid solutions which result in the more tangent loss and lower dielectric constant.

#### 4. Conclusion

The solid solution  $(\text{Ba}_5\text{TbTi}_3\text{V}_7\text{O}_{30})_x(\text{BiFeO}_3)_{1-x}$  for all values of  $x$  ( $x = 1$ ,  $x = 0.5$ ,  $x = 0.3$ ) shows ferroelectric transition (showing ferroelectric property). By increasing the BFO, the dielectric constant is reduced considerably, and at the same time, the loss (tangent) increases, which is as per the expected line. BFO having semiconducting properties increases the conduction in the solid solution. This is also reflected in the conductivity study i.e. activation energy increases by increasing BFO concentration. We can also conclude that the ferroelectric properties of BFO have been improved by the effect of BTTV.

#### References

- [1] A. Panigrahi, R. N. P. Choudhary, and B. N. Das, Structural properties of  $\text{Ba}_5\text{RTi}_2\text{ZrNb}_7\text{O}_{30}$  ( $R = \text{La, Nd, Sm, Eu, Gd, Dy}$ ) ceramic system, *Ind. J. Phys.* **74A** (2), 147 (2000).
- [2] A. Panigrahi, N. K. Singh, and R. N. P. Choudhary, Diffuse phase transition in  $\text{Ba}_5\text{NdTi}_{3-x}\text{Zr}_x\text{Nb}_7\text{O}_{30}$  ferroelectric ceramics, *J. Phys. Chem. Solids* **63**, 213 (2002).
- [3] P. S. Sahoo *et al.*, Structural and dielectric properties of  $\text{Ba}_2\text{Sr}_3\text{SmTi}_3\text{V}_7\text{O}_{30}$ , *Mod. Phys. Lett. B* **22** (30), 2999 (2008).
- [4] K. Kathayat *et al.*, Effect of holmium doping in  $\text{Ba}_5\text{RTi}_3\text{V}_7\text{O}_{30}$  ( $R = \text{rare earth element}$ ) compound, *Integr. Ferroelectr.* **118** (1), 8 (2010). DOI: [10.1080/10584587.2010.489461](https://doi.org/10.1080/10584587.2010.489461).
- [5] A. Laha, and S. B. Krupanidhi, Growth and characterization of excimer laser-ablated  $\text{BaBi}_2\text{Nb}_2\text{O}_9$  thin films, *Appl. Phys. Lett.* **77** (23), 3818 (2000). DOI: [10.1063/1.1329858](https://doi.org/10.1063/1.1329858).
- [6] Y. Wu *et al.*, Processing and properties of strontium bismuth vanadate niobate ferroelectric ceramics, *J. Am. Ceram. Soc.* **84** (12), 2882 (2001). DOI: [10.1111/j.1151-2916.2001.tb01109.x](https://doi.org/10.1111/j.1151-2916.2001.tb01109.x).
- [7] B. J. Kalaiselvi, R. Sridarane, and R. Murugan, Dielectric properties of  $\text{Sr}_{1-x}\text{B}_2\text{O}_7$  ( $x = 0.1$  and  $0.2$ ) ceramics, *Ceram. Int.* **32** (4), 467 (2006). DOI: [10.1016/j.ceramint.2005.03.026](https://doi.org/10.1016/j.ceramint.2005.03.026).
- [8] P. L. Deepti, S. K. Patri, and R. N. P. Choudhary, Frequency and temperature dependent electrical properties of magnesium bismuth vanadate, *Ferroelectrics* **540** (1), 145 (2019). DOI: [10.1080/00150193.2019.1611102](https://doi.org/10.1080/00150193.2019.1611102).
- [9] H. Doley, A. Panigrahi, and P. Chakraborty, Study of electrical and magnetic properties of multiferroic composite  $(\text{BiFeO}_3)_x(\text{Ba}_5\text{RTi}_3\text{V}_7\text{O}_{30})_{1-x}$ , *Adv. Intell. Syst. Comput.* **862**, 451 (2019).
- [10] M. Fiebig, Revival of the magnetoelectric effect, *J. Phys. D: Appl. Phys.* **38** (8), R123 (2005). DOI: [10.1088/0022-3727/38/8/R01](https://doi.org/10.1088/0022-3727/38/8/R01).
- [11] Y. N. Venetsev *et al.*, Crystal chemical studies of substances with perovskite type structure and special dielectric properties, *Sov. Phys. Crystallogr.* **4**, 538 (1960).



- [12] G. Smolenskii *et al.*, Ferroelectrics of the oxygen octahedral type with layered structure, *Sov. Phys. Solid State* **2**, 2651 (1961).
- [13] C. Michel *et al.*, The atomic structure of BiFeO<sub>3</sub>, *Solid State Commun.* **7** (9), 701 (1969). DOI: [10.1016/0038-1098\(69\)90597-3](https://doi.org/10.1016/0038-1098(69)90597-3).
- [14] J. M. Moreau *et al.*, Ferroelectric BiFeO<sub>3</sub> X-Ray and neutron diffraction study, *J. Phys. Chem. Solids* **32**, 1351 (1971).
- [15] M. M. Kumar, A. Srinivas, and S. V. Suryanarayana, Structural property relations in BiFeO<sub>3</sub>/BaTiO<sub>3</sub> solid solutions, *J App. Phys.* **87** (2), 855 (2000). DOI: [10.1063/1.371953](https://doi.org/10.1063/1.371953).
- [16] A. Dutta, and T. P. Sinha, Dielectric relaxation in perovskite BaAl(1/2)Nb(1/2)O<sub>30</sub>, *J. Phys. Chem. Solids* **67** (7), 1484 (2006). DOI: [10.1016/j.jpcs.2006.02.002](https://doi.org/10.1016/j.jpcs.2006.02.002).
- [17] P. S. Sahoo *et al.*, Structural, dielectric, electrical and piezoelectric properties of Ba<sub>4</sub>SrRTi<sub>3</sub>V<sub>7</sub>O<sub>30</sub> (R = Sm, Dy) ceramics, *Central Eur. J. Phys.* **6**, 844 (2008).